content then increased to about 7.5 percent with the crystallization of about 40 percent (by weight) crystals, first plagioclase and hypersthene and then hornblende. Such an increase in H_2O content may also be reflected in the inversely zoned margins of many plagioclase phenocrysts. The cap of the Mount St. Helens magma body "leaked," giving rise to the cryptodome. Finally, with mounting H_2O pressure, the catastrophic eruption of 18 May 1980 occurred. The Mount Hood andesite (*12*) has a SiO_2 content of about 60 percent; the 18 May 1980 samples have a content of 64 percent. Thus, the parallels between the experimental data used here and the actual 18 May 1980 magma are tentative. This scenario envisions pressures of over 3 kbar at the time of the eruption. This is equivalent to a depth of at least 9 km, but the pressure may have been reached at much shallower depths, generating short-lived overpressures. I envision an interplay of such overpressures with tectonic events, giving rise to the pre–18 May 1980 phreatic phase and the 18 May 1980 catastrophic explosion.

The T pumice (A.D. 1800) and W pumice (A.D. 1500), products of the initial phases of the last two eruptive cycles of Mount St. Helens, also tapped initially H_2O-rich magmas (Table 2) (*13*). Analyses of melt inclusions in a sample from Goat Rocks dome (T cycle) show the same low H_2O contents as in the current sequence and thus also reflect the emplacement of highly crystallized viscous, H_2O-poor magmas. The pre–18 May 1980 summit dome samples (part of W-cycle eruptives) examined so far have proven unsuitable for electron microprobe analyses. They have undergone extensive hydrothermal alteration, resulting in crystallization and compositional alteration of melt inclusions.

WILLIAM G. MELSON
Department of Mineral Sciences, Smithsonian Institution, Washington, D.C. 20560

References and Notes

1. P. W. Lipman, D. R. Norton, J. E. Taggart, Jr., E. L. Brandt, E. E. Engleman, *U.S. Geol. Surv. Prof. Pap. 1250* (1981), p. 631.
2. K. V. Cashman and J. E. Taggart, *Science* **221**, 1385 (1983).
3. W. G. Melson and C. A. Hopson, *U.S. Geol. Surv. Prof. Pap. 1250* (1981), p. 641.
4. C. H. Nielsen and H. Sigurdsson [*Am. Minerol.* **66**, 547 (1981)] described a method involving supercooling of the thin section to avoid volatilization during electron microprobe analysis.
5. A. T. Anderson, *Geol. Soc. Am. Bull.* **85**, 1485 (1974). Water contents are suggested by the deficiencies in the sums of the melt inclusions of Table 1. Anderson believes such deficiencies are a good indicator of volatile concentrations. Repeated analyses of obsidians with H_2O contents supplied by J. Delaney confirm the value of this approach for water concentrations in excess of 2 percent (by weight). Analysis of Mount St. Helens melt inclusions show less than 0.2 percent of combined chlorine, sulfur, and fluorine, an indication that most of the sum deficiency must be due to dissolved H_2O. H. Sigurdsson, [*Eos* **63**, 601 (1982)] reported a sulfur content of about 100 ± 50 parts per million in 18 May 1980 pumice.
6. S. Hart, personal communication. This sample is analysis 3, Table 2. In this sample, melt inclusions in hornblende and plagioclase have no systematic differences in composition.
7. W. G. Melson, *Calif. Div. Mines Geol. Spec. Rep. 63* (1982), p. 111; C. Newhall and W. G. Melson, in preparation.
8. K. F. Sheidegger, A. N. Federman, A. M. Tallman, *J. Geophys. Res.* **87**, 10861 (1982).
9. J. C. Eichelberger and D. B. Hayes, *ibid.*, p. 7727.
10. H. R. Shaw, *Am. J. Sci.* **272**, 870 (1972).
11. See A. R. McBirney [*J. Volcanol. Geothermal. Res.* **7**, 357 (1980)] for mechanisms other than crystal fractionation for generating the compositional diversity of rocks erupted by calc-alkaline volcanoes.
12. D. H. Eggler and C. W. Burnham, *Geol. Soc. Am. Bull.* **84**, 2519 (1973).
13. C. A. Hopson [*Geol. Soc. Am. Abstr. Programs* **4**, 172 (1972)] first outlined Mount St. Helens eruptive sequences involving successive H_2O degassing.
14. R. L. Christiansen and D. W. Peterson, *U.S. Geol. Surv. Prof. Pap. 1250* (1981), p. 22.
15. I thank D. Swanson, C. Kienle, C. Hopson, K. Cashman, C. Heliker, and D. Dzurisin who contributed some of the samples; J. Norberg and J. Nelen who did the classical wet bulk analyses; T. O'Hearn and D. Jerez who assisted with sample preparation and drafting; E. Jarosewich who assisted with the electron microprobe analyses; D. Eggler, C. A. Hopson, A. R. McBirney, C. Merzbacker, S. McNutt, C. Newhall, D. Smith, D. A. Swanson, and T. L. Wright who reviewed and improved a draft of this report; R. Johnson and F. Walkup who prepared the polished sections used in the electron and ion probe analyses; and S. R. Hart and N. Shimizu who performed ion probe analyses of melt inclusions.

10 February 1983; revised 22 June 1983

Deep Earthquakes Beneath Mount St. Helens: Evidence for Magmatic Gas Transport?

Abstract. *Small-magnitude earthquakes began beneath Mount St. Helens 40 days before the eruption of 20 March 1982. Unlike earlier preeruption seismicity for this volcano, which had been limited to shallow events (less than 3 kilometers), many of these earthquakes were deep (between 5 and 11 kilometers). The location of these preeruptive events at such depth indicates that a larger volume of the volcanic system was affected prior to the 20 March eruption than prior to any of the earlier dome-building eruptions. The depth-time relation between the deep earthquakes and the explosive onset of the eruption is compatible with the upward migration of magmatic gas released from a separate deep reservoir.*

Volcanic earthquakes have been used as the basis for eruption prediction at many volcanoes. Predictions typically are based on either the rapid increase in the number of shallow, small-magnitude earthquakes or the upward migration of earthquake locations to shallower depths (*1, 2*). At Mount St. Helens, all the eruptions since the renewal of activity in March 1980 have been preceded by swarms of shallow earthquakes, harmonic tremor, or both (*2–4*). Neither earthquakes deeper than 5 km nor evidence of the upward migration of seismic foci were observed prior to any eruption of this volcano before 1982.

The eruption of Mount St. Helens on 20 March 1982 was preceded by shallow volcanic earthquakes, but there were two distinct differences from the sequence of events observed in earlier dome-building eruptions. First, the increase in seismicity began well in advance of either changes in geodetic measurements or tilting of the crater floor near the lava dome (*5, 6*). This contrasts with the observations of the 1981 dome-building eruptions, when measured distances between points near the lava dome and a fixed reference point showed significant acceleration in the rate of contraction before the number of shallow volcanic earthquakes began to increase above the background frequency (*4, 5*). Second, this was the first eruption of Mount St. Helens preceded by deep earthquakes (depth, > 5 km). The 1980 explosive eruptions were followed by swarms of deep earthquakes (*3*); the other dome-building eruptions were neither preceded nor followed by deep earthquakes that could be related to the eruption.

The seismic network at Mount St. Helens includes six stations on the immediate cone and ten stations at distances out to 40 km. The data are recorded on an event-triggered digital computer system. The large number of stations on the mountain and the fine resolution of the digital data permit accurate determination of earthquake locations beneath the crater. The velocity model is a modification of one developed for the Cascade Range (*7*). The hypocenters for a total of 493 earthquakes beneath Mount St. Helens between 1 February and 23 March 1982 were calculated. Data for 262 well-recorded events were included in this study (*8*).

The shallow preeruption earthquakes are centered near the lava dome (Fig. 1); similar patterns have been observed before all the other dome-building eruptions and two of the 1980 explosive eruptions (*3*). The shallow volcanic earthquakes have coda magnitudes of less than 3.0, and they cluster in the upper 3

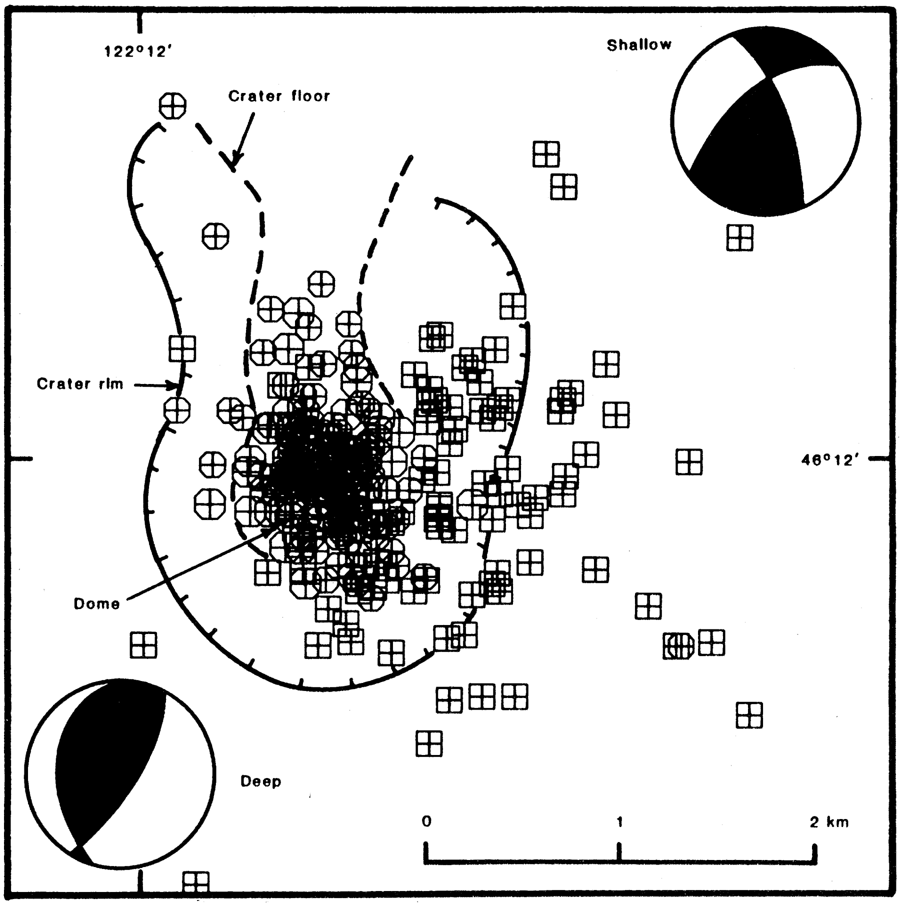

Fig. 1. Distribution of epicenters beneath the Mount St. Helens crater area. Earthquakes are scaled according to magnitude: the smallest symbols represent earthquakes with magnitudes less than 1.0; the largest symbols, magnitudes greater than 2.0. Circles represent earthquakes shallower than 5 km and squares represent earthquakes deeper than 5 km. The composite focal mechanisms are upper hemisphere: white quadrants represent dilation and darkened quadrants compression.

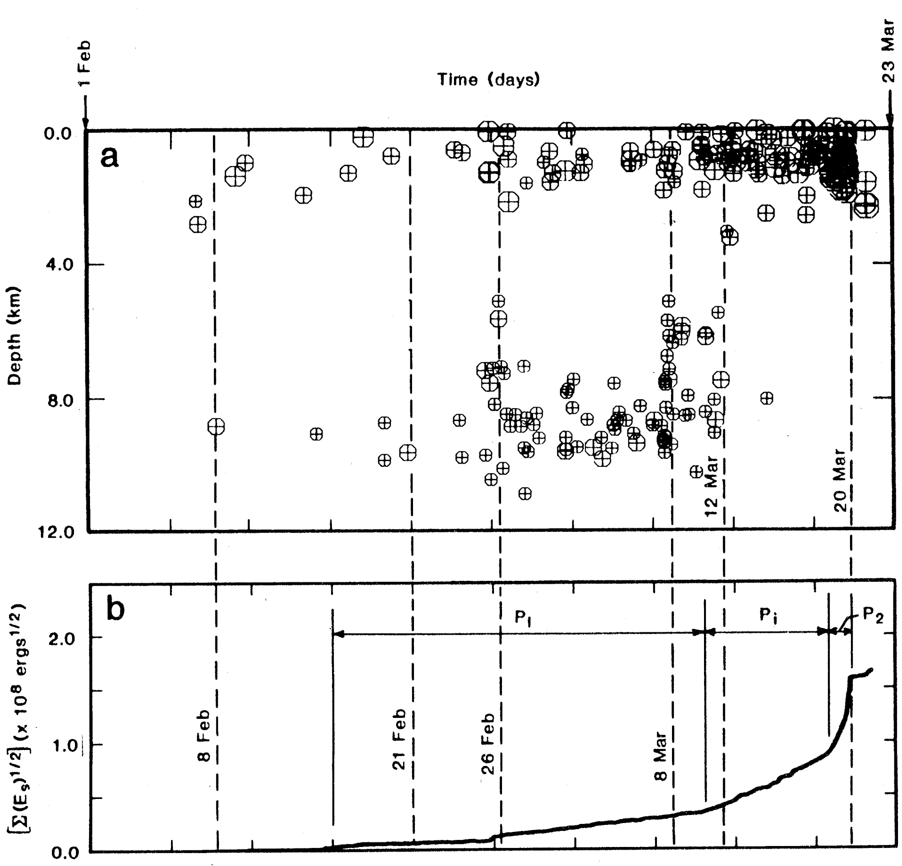

km (Fig. 1). A composite focal mechanism for four of the larger magnitude earthquakes of late February is consistent with strike-slip faulting with a small thrust component. The nodal planes strike northeast and northwest (Fig. 1).

The deep earthquakes have magnitudes of less than 1.0, and their epicenters are distributed over a larger area than those of the shallow earthquakes (Fig. 1). The plot of the earthquake distribution has a distinct gap between depths of 3 and 5 km (Fig. 2a). The focal mechanisms of the deep earthquakes appear to belong to two major classes. A well-constrained composite focal mechanism for ten deep earthquakes reveals thrust faulting along north-northeast–striking nodal planes (Fig. 1). The second class of mechanisms is poorly defined but appears to involve nearly vertical strike-slip faulting with the strike of the nodal planes northeast and northwest, similar to the shallow composite mechanism.

The first deep earthquake before the eruption of 20 March 1982 was detected on 8 February. Between 8 and 21 February, five deep earthquakes occurred (at depths of 9 km) and eight shallow quakes occurred (above 3 km). For the next 20 days, the number of locatable deep earthquakes was larger than the number of locatable shallow earthquakes (Fig. 2a), although the energy released by the shallow quakes was greater. During one 8-hour period on 8 March, the deep earthquakes showed an upward migration (Fig. 2a): earthquakes shallowed nearly monotonically from an average depth of 8 to 9 km to about 4.5 to 5.0 km—an average upward progression of hypocenters of more than 0.5 km/hour. Another possible episode of upward migration occurred on 26 February, although the earthquake hypocenters then did not shallow monotonically (Fig. 2a).

In the course of a given preeruptive episode at Mount St. Helens, seismic energy is released at an increasing rate. The release of seismic energy for most dome-building eruptions can be divided into two phases. During phase 1, which lasts from a week or more to a few days

Fig. 2. (a) Depth-time plot. Earthquakes are scaled according to magnitude as in Fig. 1. Tick marks on the time axis indicate 5-day increments starting on 1 February 1982 and ending on 23 March 1982. The dashed vertical lines indicate dates discussed in the text. (b) Plot of the accumulated square root of released seismic energy, $(E_s)^{1/2}$, versus time; P_1, P_2, and P_i indicate the first phase, second phase, and intermediate phase of accumulated $(E_s)^{1/2}$. The curve includes all known earthquakes at Mount St. Helens, not just the reliably located events.

before the eruption, the square root of released seismic energy $[(E_s)^{1/2}]$ accumulates at a near-constant rate (*9*). Phase 2, which corresponds to the few days immediately before the eruption, is marked by an abrupt increase in $(E_s)^{1/2}$. The rate of increase of the accumulated $(E_s)^{1/2}$ during phase 1 has shown little variation among the individual eruptive episodes, and the sizes of the step increases in phase 2 have been within a factor of about 4 (*9*). The eruption of 20 March 1982 had a well-defined intermediate phase that began about 12 March (Fig. 2b), just as the deep earthquakes were ending; its intermediate phase lasted about 6 days and ended with an abrupt increase on the day before the eruption (Fig. 2b).

Our interpretation of the seismic data is as follows. The earthquake locations and focal mechanisms support the hypothesis that there is a northeast-striking fault (*10*) located just north of the lava dome (Fig. 3). The thrust and strike-slip focal mechanisms along the fault suggest that the maximum principal stress direction is northwest-southeast. Since the regional principal stress direction in southwestern Washington is northeast-southwest, we interpret the rotated stress direction near the lava dome to be the result of volcanic pressures associated with the magmatic system (Fig. 3). On the basis of the earthquake-depth distribution (Fig. 2), we divide the subsurface volcanic system into a shallow part and a deep part, with the point of separation located at the depth of the seismic gap (Fig. 3). The hypocenter gap could be caused by a volume (possibly a partial melt) that supports little stress or, alternatively, is of high strength. The shallow system probably includes the remnant of a magma body emplaced on 18 May 1980 that remained isolated from the deeper system until 1982 (*11*). The deep earthquakes are the first evidence since 1980 of the existence of the deep reservoir.

Assuming that the deep earthquakes are related to the subsequent eruption, we suggest the following model for the March 1982 eruptive episode. Increases in fluid pressure in the deep system (5 to 11 km) caused brittle failure—that is, earthquakes, in the surrounding country rock. These earthquakes occur preferentially on an existing northeast-striking fault, along which the breaking strength is more easily exceeded (Fig. 3). The time-depth relation (Fig. 2a) implies that after 21 February these increasing fluid pressures must have been large enough to cause failure in a significant volume (~ 10 km^3) of the country rock. When fluid pressure reached a critical value, fluid transport from the deep system to the shallow reservoir was initiated so that new fluid was injected into the shallow system. This fluid transport increased the fluid pressure in the shallow volcanic system, the effects of which were first observed as the intermediate phase in the accumulating sum of $(E_s)^{1/2}$ (Fig. 2b). As additional fluid was delivered to the shallow system, increasing fluid pressure continued to increase the volcanic stresses, which in turn initiated shallow volcanic earthquakes of increased magnitude. On 12 March, fluid pressure in the deep system had dropped enough that earthquakes stopped below 5 km. This fluid-transfer process culminated on 20 March, when fluid pressure immediately below the dome finally exceeded the breaking strength of the dome and a small explosive eruption resulted.

In view of the relevant petrologic and geodetic data, we postulate that for the 20 March 1982 eruption magmatic fluid was transferred from the deep reservoir to the shallow reservoir in the form of volatiles that had been separated from the magma of the deep reservoir. Geodetic and tilt observations indicated that for this eruption deformation occurred only in the immediate vicinity of the lava dome (*5*); there is no evidence of a major intrusion of magma into the shallow reservoir. The petrologic changes that might be expected if new magma had entered the shallow reservoir were not observed in the products that erupted either in March or in the subsequent dome-building eruptions of April, May, and August 1982 (*12*). An increased level of gas emissions, relative to those of earlier dome-building eruptions, was noted after the March and April eruptions (*13*). This observation could be due to the increased volatile supply.

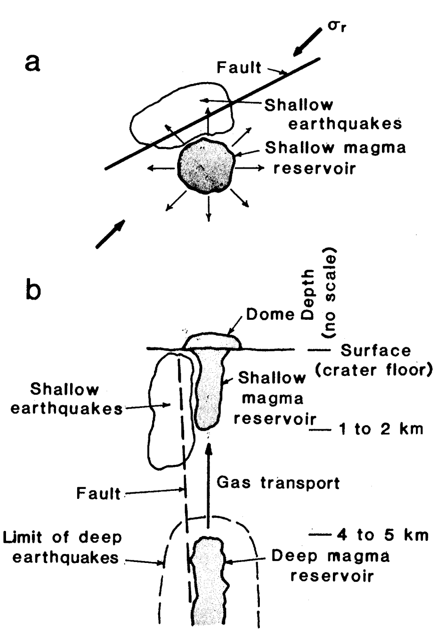

Fig. 3. Simple model of the Mount St. Helens subsurface volcanic system, developed on the basis of seismic data. (a) Plan view showing the relation among the northeast-striking fault, lava dome, and shallow-earthquake hypocenters. The large arrows represent the direction of the regional maximum principal stress, and the small arrows represent the postulated volcanic pressure. (b) Cross section showing the postulated relation between the shallow and deep volcanic reservoirs, the fault zone, and the earthquakes.

The patterns of occurrence of deep and shallow earthquakes preceding the eruption of 20 March 1982 has implications for both hazard assessment and monitoring at Mount St. Helens. First, the occurrences of deep earthquakes indicate that a larger volume of the volcanic system was involved than in any of the earlier dome-building eruptions. Assessments of volcanic hazards for any future eruption will need to consider the possibility that renewed activity of the deep reservoir is involved. Second, seismic data for March 1982 indicate that the processes controlling fluid pressures in the deep reservoir are independent of the controlling processes in the shallow reservoir. For the March 1982 eruption, only the seismic monitoring detected differences between the precursory patterns for that episode and those preceding the other dome-building eruptions; none of the other geophysical monitoring techniques used in the crater detected unusual observations for the 20 March eruption that could be related to physical changes in the deep system (*5, 6, 12, 13*). To ensure that changes in the deep system are not overlooked, it is imperative that seismic monitoring activities continue outside the crater. Third, the record from March 1982 and the small magnitudes (< 1.0) of the deep earthquakes detected should be viewed as a warning that, despite the similar precursors observed before the other dome-building eruptions, the deep system conceivably could influence a future eruption with no apparent precursory manifestations in any of the geophysical monitoring procedures—geodetic, gas emission, or seismic. Finally, the occurrence of deep earthquakes in future preeruption sequences should be viewed as a warning of the possible occurrence of fluid transport and, with it, of the increased probability that the forthcoming eruption will have an explosive component.

CRAIG S. WEAVER

U.S. Geological Survey at University of Washington, Seattle 98195

JAMES E. ZOLLWEG

STEPHEN D. MALONE

Geophysics Program, University of Washington

References and Notes

1. T. Minakami, in *Physical Volcanology*, vol. 6 of *Developments in Solid Earth Geophysics*, L. Civetta, P. Gasparini, G. Luongo, A. Rapolla, Eds. (Elsevier, Amsterdam, 1974), pp. 313–333; D. Shimozuru, in *The Surveillance and Prediction of Volcanic Activity* (Unesco, Paris, 1972), pp. 19–45.
2. S. D. Malone, E. T. Endo, C. S. Weaver, J. W. Ramey, *U.S. Geol. Surv. Prof. Pap. 1250* (1981), p. 803.
3. C. S. Weaver, W. C. Grant, S. D. Malone, E. T. Endo, *ibid.*, p. 109.
4. S. D. Malone, C. Boyko, C. S. Weaver, *Science* **221**, 1376 (1983).
5. W. W. Chadwick, Jr., D. A. Swanson, E. Y. Iwatsubo, C. C. Heliker, T. A. Leighley, *ibid.*, p. 1378.
6. D. Dzurisin, J. A. Westphal, D. J. Johnson, *ibid.*, p. 1381.
7. The velocity model at Mount St. Helens has a surface layer with a velocity of 3.8 km/sec and a thickness of 1.0 km overlying a 1-km-thick layer with a velocity of 4.6 km/sec and a 1-km-thick layer with a velocity of 5.0 km/sec. Below 3 km, the velocity model is similar to the regional Cascade Range velocity model discussed by W. M. Kohler, J. H. Healy, and S. S. Wegener [*J. Geophys. Res.* **87**, 339 (1982)].
8. All the earthquakes examined in this study have at least seven well-recorded P-wave arrivals, root-mean-square travel time residuals of less than 0.25 second, and calculated errors of less than 1.5 km in all three dimensions. The actual resolution of the hypocenters for the shallow volcanic earthquakes (depths < 2.5 km) is about 1 km.
9. The calculation of seismic energy released at Mount St. Helens is discussed by Malone *et al.* (*4*). These investigators consider the problems of identifying changes in the shape of the energy release curve but do not explicity divide the accumulated $(E_s)^{1/2}$ curve into the two phases discussed here. Both the initial constant increase and the final step increase phase discussed here are clearly evident for most of the nine eruptions plotted in figure 2 of (*4*).
10. The scarp mapped immediately north of the lava dome [figures 2 and 3 of (*5*)] may be the surface expression of the fault hypothesized in our model on the basis of the earthquake locations and focal mechanisms.
11. A number of investigators have proposed that a shallow magma body was emplaced during the cataclysmic eruption on 18 May 1980 [P. W. Lipman, D. R. Norton, J. E. Taggart, Jr., E. L. Brandt, E. E. Engleman, *U.S. Geol. Surv. Prof. Pap. 1250* (1981), p. 631].
12. K. V. Cashman and J. E. Taggart, *Science* **221**, 1385 (1983).
13. T. Casadevall *et al.*, *ibid.*, p. 1383.

14. We appreciate the many hours that S. Carlson and J. Terreberry worked in support of the prediction effort during the eruption sequence of February to March 1982 and the assistance of W. Grant in the reexamination of the earthquake data.

26 January 1983; revised 27 June 1983

Eruption-Triggered Avalanche, Flood, and Lahar at Mount St. Helens—Effects of Winter Snowpack

Abstract. *An explosive eruption of Mount St. Helens on 19 March 1982 had substantial impact beyond the vent because hot eruption products interacted with a thick snowpack. A blast of hot pumice, dome rocks, and gas dislodged crater-wall snow that avalanched through the crater and down the north flank. Snow in the crater swiftly melted to form a transient lake, from which a destructive flood and lahar swept down the north flank and the North Fork Toutle River.*

Since the explosive eruptions of Mount St. Helens in 1980 (*1*), dacitic lava has erupted periodically to build a dome that in early 1982 rose some 200 m above the crater floor (Fig. 1). On 19 March 1982, a dome-building eruption began with an explosive phase. Had the eruption occurred in summer, the destructive effects of the relatively small explosive eruption would have been confined to the crater and the upper flanks of the volcano. But because snow thickly mantled the steep crater wall, a lateral blast generated a large avalanche that flowed 8 km off the volcano. Heat from eruption products meanwhile swiftly melted snow, producing a transient lake whose sudden discharge extended effects of the eruption far downvalley. The complex sequence of eruptive and flow events—probably all occurred within a few minutes—are inferred from stratigraphic field relations gathered within a few days of the eruption and from geophysical data and distant visual observations.

Glowing projectiles were observed above the crater rim from an aircraft 35 km south of the volcano at about 1927 P.S.T. (0027 U.T., 20 March), roughly the time of the seismic onset of the eruption (*2*). The projectiles apparently were part of a blast of hot juvenile pumice, dome rocks, and gas that erupted from the south side of the dome. Two or 3 minutes later, a central eruption column rose to an altitude of 13.6 km (*3*); wind carried the plume southeast, depositing pumice on the southeast flank of the volcano and beyond. The absence of pumice on the dome indicates that both the lateral blast and the vertical column were directed away from the dome, probably from a vent low on its south flank or adjacent crater floor (*4*).

The lateral blast dislodged most of the snow from the precipitous, 500-m-high crater wall in the 120° sector east through south-southwest. The snow and injected rocks avalanched down the steep wall. Snow that remained high on the crater wall after the eruption was studded with angular blocks; snow remaining near the base of the wall had become deeply fluted and grooved by the avalanche.

The avalanche split and flowed around both sides of the dome, joined 400 m farther north in the axis of the breach, descended the north flank of the volcano, and swept across the pumice plain to Spirit Lake and the North Fork Toutle River (Figs. 1 and 2). The volume of the avalanche was 10^6 to 10^7 m^3. Its velocity, calculated from run-up and superelevation of deposits (*5*), varied with slope and with distance from the crater. The avalanche accelerated down the crater wall to about 70 m/sec. Running down the gentle crater floor and breach, the avalanche gradually slowed to 10 m/sec but then accelerated to about 16 m/sec as it descended the steps and north flank of the cone. On the pumice plain it slowed to 6 m/sec and less. The maximum distance traveled was 8.4 km; the approximate center of mass was displaced 5.5 km. The fahrböschung (*6*) was about 9°, suggesting an average apparent coefficient of friction of about 0.16.

Along its axis the avalanche eroded through the snowpack in the breach and into pumice and rockfall deposited in 1980 and 1981. But near its lateral margins the avalanche was much less erosive; locally it plowed up large snow blocks, but in general it barely disturbed the snow, over which it laid deposits 0.1 to 1 m thick. In a few places near its margins, the avalanche descended into fumarole-melted caves in the snowpack. After descending the steps, the avalanche decelerated and spread out on the pumice plain, depositing snow and lithic debris as thick as 3 m over several square kilometers. The margins of the deposits were steep-fronted lobes 0.3 to 1 m high, where pumice blocks were concentrated.

The avalanche deposit typically was a nonsorted, nonstratified mixture, half corn-snow granules and half pumice and rock fragments. Downslope it was progressively enriched in rock fragments, owing to the incorporation of scoured material. The poorly sorted fragments of pumice and rock, ranging from clay to boulder size, made the deposit dark gray (Figs. 1 and 2). The initial porosity of the deposit was about 40 percent; the 1-mm median grain size of snow granules in the avalanche deposit was similar to that of undisturbed snow in the crater. Weeks later when the snow had melted, the deposit had settled to a nonsorted, nonstratified, light-gray, dry, pumiceous sandy gravel only 1 cm to 1 m thick.

Certain characteristics of the deposit before its snow component had melted suggest that the avalanche behaved variously as a dry flow and as a brittle slide. The thinness of the distal deposit, its lobate form, the concentration of large low-density blocks at the margins, and the long runout distance suggest a dominantly dry-flow style of movement (*7*).